Airborne Nanoparticle Release Associated with the Compounding of Nanocomposites using Nanoalumina as Fillers

Su-Jung (Candace) Tsai*, Ali Ashter, Earl Ada, Joey L. Mead, Carol F. Barry, Michael J. Ellenbecker

NSF Center for High-rate Nanomanufacturing (CHN), University of Massachusetts Lowell, One University Avenue, Lowell MA 01854 USA

Abstract

Twin screw extrusion is the preferred process to commercially produce nanocomposites by compounding the nanoparticles and polymer melts. Polymer nanocomposites, which contain nanoparticles dispersed in a polymer matrix, provide improved properties at low filler loadings. Nanoalumina particles recently have been used as fillers to polymer matrix that contributed enhanced physical properties of nanocomposites. Recently, concerns had been expressed that airborne nanoparticles particularly of nanoalumina released during compounding might present serious contamination of the air in the workplace. Researchers with experience in environmental health and polymer manufacturing monitored the compounding process for a model nanoalumina-containing nanocomposite using a TSI Fast Mobility Particle Spectrometer (FMPS). FMPS measurements were taken at background locations, source locations, and operators' breathing zones; in parallel to the FMPS real time measurement, airborne nanoparticles were collected using polycarbonate filters fitted with filmed grids driven by a personal air sampling pump. Filter samples were analyzed for particle morphology and elemental composition. It was found that the nanoparticle number concentration was elevated during processing. The released nanoparticles are a complex mixture of the individual nanoalumina particles, agglomerates of those particles, polymer fume particles, and perhaps others.

Keywords: Airborne nanoparticles; Nanoalumina; Nanocomposite compounding; Nanoparticle mobility size; Twin screw extruder (TSE).

INTRODUCTION

Polymers are often reinforced using a second inorganic or organic phase; traditionally, micrometer-sized particles have been used as the filler. In polymer nanocomposites these fillers have at least one dimension less than 100 nm (Kojima *et al.*, 1993). These fillers include alumina, carbon black, silica, talc, calcium carbonate, layered

Corresponding author. Tel.: +1-978-934-4366; Fax: +1-978-934-3050

E-*mail address:* candace.umass@gmail.com

silicates (nanoclays), and recently, silver and engineered nanoparticles such as carbon nanotubes. Although the nanometer-sized particles allow low filler loadings (< 10%$_w$) in nanocomposites with a retention of flexibility and impact properties, the resulting nanocompound's properties are highly dependent on dispersion of the primary filler particles through the polymer matrix. With good dispersion, each particle is wetted completely by the melted polymer, creating a very high interfacial surface area that can improve properties of the polymer (McCarrie and Winter, 2003).

Since commercial compounding (mixing) of nanocomposites is typically achieved by feeding the nanoparticles and polymer into a twin screw extruder, the airborne particles associated with nanoparticle reinforcing agents are of particular concern, as they can readily enter the body through inhalation. Recent research has suggested that nanometer-sized particles of many materials, including nanoalumina, display greater toxicity than for larger particles, and aggregated nanoparticles can be deaggregated in the lung after inhalation (Ferin *et al.*, 1991; Wolff *et al*., 1988; Zhang *et al*., 2000; Renwick *et al*., 2004; Warheit, 2004). In addition, Maynard *et al.* (2005) concluded that aerosol control methods have not been well-characterized for nanometer-sized particles, although theory and limited experimental data indicate that conventional ventilation, filtration, and other engineering control approaches should be applicable in many situations.

Consequently, researchers with experience in occupational and environmental health and melt compounding of polymer nanocomposites investigated the magnitude of exposures to airborne nanoparticles associated with the commercial compounding of nanocomposites. A series of twin screw extrusion trials presented in this study was monitored during fall 2006 and spring 2007. Three sets of data monitored under similar conditions were selected for presentation here. The filler used for this compounding process was nanoalumina particles; other fillers were not used for this study. We studied characteristics of nanoparticle release, agglomeration, and transport in the compounding workplace.

METHODS

Materials, equipment and compounding process

Model nanocomposite systems consisting of nano-aluminum oxide (nanoalumina) and polymethylmethacrylate (PMMA) were employed in this study. The nano-aluminum oxide (Al_2O_3) obtained from Nanophase Technologies Corporation (grade Al-015-003-025) was manufactured using physical vapor synthesis (PVS). The nanoalumina particles were roughly spherical in shape with an average primary particle size ranging from 27-56 nm and a reported density of 3600 kg/m^3.[1] When dried, these particles formed agglomerates in the bulk material with a nominal size of 200 nm. The extrusion-grade polymer resins were

[1] Technical information retrieved from Nanophase website, http://www.nanophase.com/technology/capabilities.asp

selected for their partial compatibility with the nanoalumina particles and their stability during melt processing. Each trial used 2.3 kg of polymer pellets and 0.16 kg of nanoalumina particles. Nanoalumina particles were dried at 170°C continuously for 8 h prior to each trial.

Standard industrial equipment including a 30-mm co-rotating twin screw extruder (TSE, Werner & Pfleiderer, Model: ZSK-30) with a strand die, a single screw volumetric feeder, a twin screw volumetric feeder, a water bath, and a belt puller were used to compound polymer nanocomposites. During the twin screw extrusion process, the polymer pellets and nanoalumina particles were fed into the twin screw extruder where the polymer is melted and then mixed with the filler. The twin screw extrusion was heated above 200°C for each trial. The mixed melt was then forced through the die, forming a strand. This strand was then cooled and solidified as it was pulled through the water bath by the belt puller. Strand pelletizing equipment, which is typically attached to the line, was not used during most of the monitored trials (the strands were pelletized in a separate step).

As shown in Fig. 1, the twin-screw extruder consists of two co-rotating screws in a metal barrel which contains heating elements and water cooling. This extruder has three feed or vent ports. Typically, polymer particles are fed from a single screw volumetric feeder into the feed port nearest the drive end of the screw. The polymer is melted by shearing elements in the first sections of the screws, allowing filler material fed from a twin screw volumetric feeder into the first or second (middle) feed port to contact molten polymer. The polymer and filler is mixed between the second and third port, with the third port being available for venting of volatiles. In the experiments reported in this study, the polymer and nanoalumina were fed separately into the first port using a single screw volumetric feeder for the polymer and a twin screw volumetric feeder (with a stirrer) for the nanoalumina.

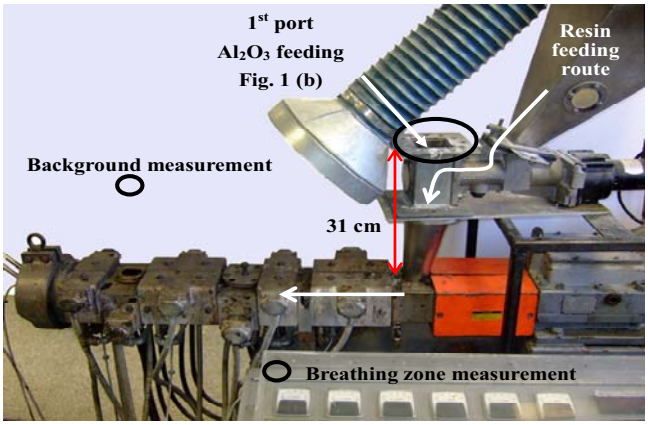

Fig. 1. (a) Layout of twin screw extruder and measurement locations.

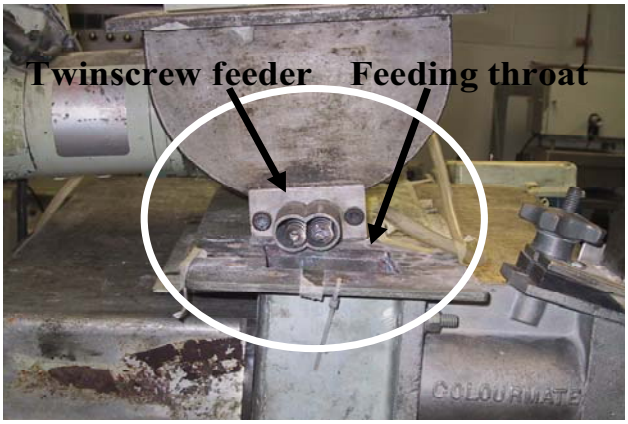

Fig. 1. (b) Close-up of the twin screw feeder & feeder port.

A feeding tunnel was connected to the feed throat to smoothly load nanoparticles. As illustrated in Fig. 1, a local exhaust system had been installed on the TSE to help control

contaminants given off by the process. It consists of a 30 cm (12 in.) diameter round hood connected to a flexible duct, with an exhaust air flow of 100 m^3/h (60 ft^3/min). During these experiments, the hood was positioned 30 cm (12 in.) above the extruder to collect polymer fumes given off from the melted mixture of polymer and nanoalumina; it was not placed near the feeding port.

A typical operation of compounding process includes five time periods as illustrated in Fig. 2(a). During phase I, the warm up period, the TSE was warmed up from room temperature to above 200°C. Phase II is for setup and calibration, when nanoalumina particles were loaded from the twin screw feeder to calibrate the feeding rate. Phase III is for compounding of virgin polymer; when polymer pellets but no nanoalumina particles were loaded into the extruder from the hopper. Phases IV and V are for compounding of nanocomposites, when nanoalumina particles were fed by a twin screw feeder into the extruder in parallel with feeding polymer pellets through port No. 1; in Phase IV, 2% nanoalumina by weight was fed and 5% nanoalumina was fed in Phase V.

Particle measurement

The concentrations of airborne nanoparticles were measured by the Fast Mobility Particle Sizer (FMPS™) spectrometer (Model 3091, TSI) in the range from 5.6-560 nm, offering a total of 32 channels of resolution (16 channels per decade). The FMPS spectrometer performs particle size classification based on differential electrical mobility classification. The FMPS is calibrated and certified by the manufacturer to give total number concentration within ± 20% of actual value; and it gives measured particle size within ± 10% of actual size. In addition, the particle size response from the FMPS was calibrated in our laboratory with test aerosols consisting of 20, 40, 100, and 200 nm of polystyrene latex spheres.

Measurements were taken starting with the warm-up of the twin screw extruder and continued until nanocomposite compounding was completed. Measurement locations included a background location, a source location, and researchers' breathing zone (Fig. 1(a)). A three-meter length Tygon® tubing was connected to the air inlet of FMPS to reach the measurement locations.

Background concentration is defined as the particle number concentration (particles/cm^3) in the air of the lab measured before, during and after the experiments. The detecting location of the background concentration was 55cm (22in.) behind the 3rd port (4th zone) of the TSE (see Fig. 1(a)). Background concentration was measured before the experiments began (measurement (1) in Fig. 2(a)); this is the general lab background before any nanoparticles are generated by operating the TSE. The background measurement was repeated after the TSE was warmed up to its operating temperature; measurement (2) was taken at this time. The third background concentration measurement was taken while feeding 5% nanoalumina, and the fourth and final background sample was collected at the end of the experiment.

Breathing zone concentration is defined as the particle number concentration (particles/cm^3)

at the TSE control panel. The height of the control panel is above most workers' waist height and below the neck height. The horizontal distance to the feeding port of the TSE was about 50cm (20 in.) Breathing zone concentration was only measured during feeding 5% nanoalumina (measurement No. 3).

Source concentration is defined as the particle number concentration (particles/cm^3) in the air near the feeding port. The detecting location for the source concentration was 8 cm

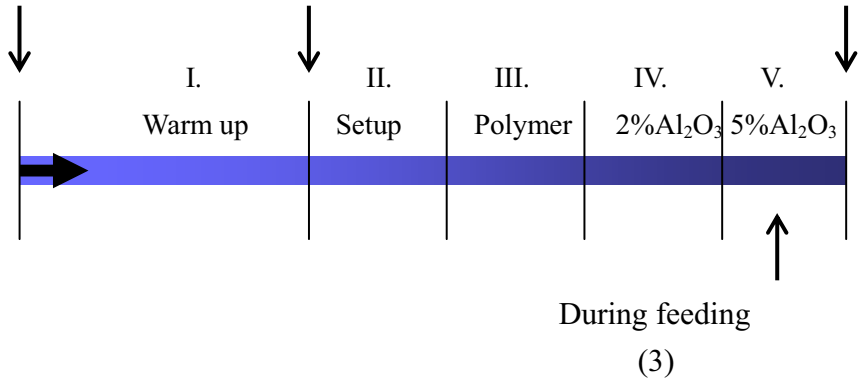

Fig. 2. (a) Illustration of the time sequence during compounding and the timing of particle measurement. Roman numerals indicate the phases of a typical experiment; numbers indicate sampling times.

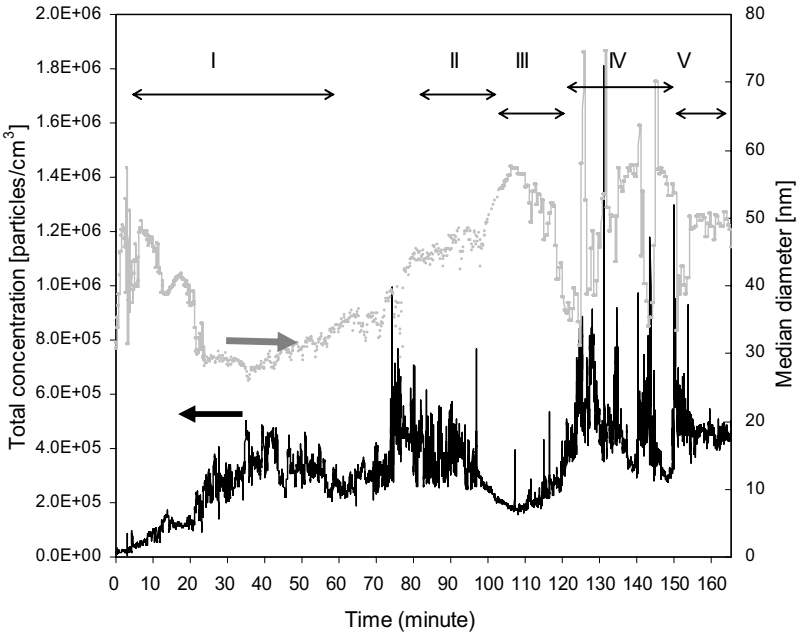

Fig. 2. (b) Total number concentration and particle median diameter at different time periods and operations of experiments. This compounding process was operated using twin screw feeder feeding in the primary feeding port (the first port).

(3 in.) from the feeding port. Source concentration also was only measured during 5% nanoalumina feeding.

Particle number concentrations normalized for channel width were calculated in each of the 32 channels for each phase of the measurement time period. Background concentration measured before feeding nanoalumina into the twin screw extruder was used as the baseline for subtraction from the various concentrations measured during processing.

The magnitude of nanoparticle exposure associated with nanoalumina compounding was measured before, during and after feeding nanoalumina particles to the compounding process. Particle size for each measurement period was evaluated by determining the particle size distribution, geometric mean, and total concentration, which were calculated by the FMPS software.

Particle sampling and characterization

A new nanoparticle aerosol filter sampler was developed and used in these experiments. A schematic layout of the sampling setup is shown in Fig. 3. TEM-copper grids (400 mesh with a titanium dioxide film) were taped on 47 mm diameter polycarbonate membrane filters (0.2 μm pore size). Fiber backing filters were used to support the polycarbonate filters. Air flow was driven by a pump at a flow rate of 1.5 L/min and 2.5 L/min for source and breathing zone locations respectively, and particles were collected on the grid for analysis. Particles were collected by diffusion onto the grid. It is recognized that particle collection favors smaller particles; this sampling was performed only to identify particle morphology and chemical composition, and not particle concentration as a function of particle size.

Scanning transmission electron microscope (STEM) images of the filter samples were collected using a field emission scanning electron microscope (JEOL, Model: JSM-7401F). The STEM images were obtained using a transmitted electron detector (TED) attachment to the scanning electron microscope and with the microscope operated at an accelerating voltage of 20 kV. Elemental analysis was performed using an energy

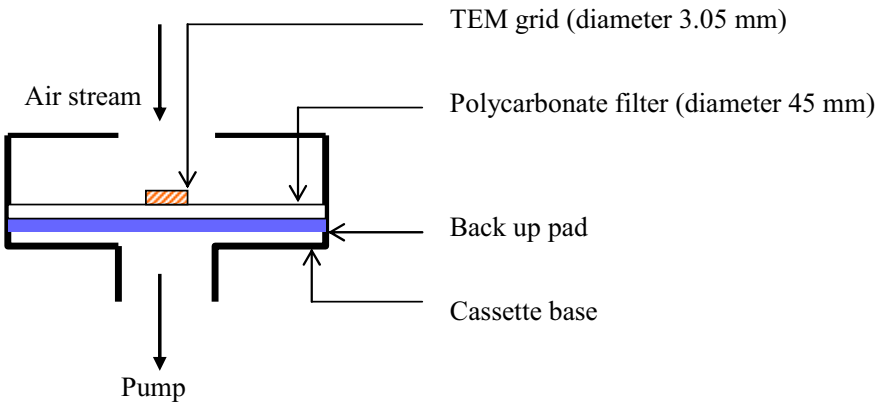

Fig. 3. Design of the TEM grid sampler.

dispersive spectroscopy (EDS) attachment of the SEM (EDAX) with a primary electron beam excitation energy of 10 kV.

RESULTS AND DISCUSSION

Changes in total particle concentration and median size

The results of one typical processing experiment performed on March 22, 2007 are presented and discussed here; in addition, two more experiments performed in November 2006 and February 2007 are presented for comparison of measurements at the source. The temporal patterns of total number concentration and median diameter are presented in Fig. 2(b). This long-term monitoring shows total number concentration measured from the beginning of warm up to the end of the operation; background concentrations were measured in the sequence shown in Fig. 2(a) while source and breathing zone concentrations were only measured during the feeding of 5% nanoalumina. During phase I, the TSE was warmed up from room temperature to above 200°C, and concentrations were measured at a central location of room background about 55 cm (22 in) from the TSE both before heating (measurement 1) and after heating (measurement 2). The laboratory door and windows were closed and the local ventilation system was on, and there were no nanoalumina particles introduced into this room during the warm up period.

As shown in Phase I of Fig. 2(b), particle median size decreased from 50 nm to values less than 30 nm after 20 min of heating, due to a large quantity of complex mixtures of nano sized fumes released from the heated extruder. During Phase II, the calibration period, the twin screw feeder of nanoalumina particles placed nearby the primary feeding port of extruder was calibrated for the feeding rate by loading nanoalumina particles into a cup. Free nanoalumina particles were introduced and released into the room and particle concentrations were measured at room background and breathing zone locations. Peaks shown in the black curve of particle total concentration seen in Fig. 2(b) were agglomerated nanoalumina particles released during the compounding process. Meanwhile, the particle median size shown by the light gray curve of Fig. 2(b) gradually increased to above 40 nm at the end of Phase II due to the larger size of the agglomerated nanoalumina particles that were released.

Phase III represents the first step of the compounding process, when the virgin PMMA polymer was loaded into the extruder. Concentrations were measured at room background, breathing zone and source location. Particle median sizes dropped to close to 30 nm. This was likely due to the absence of any agglomerated nanoalumina being fed and the formation of very small polymer fume particles when the polymer pellets were dropped into the heated extruder through the feeding throat.

During Phases IV and V, nanoalumina particles were loaded at 2% and 5% weight of polymer (PMMA) respectively in parallel with loading PMMA pellets. The peak total concentrations at the source were on the order of 10^6 particles/cm^3, and the particle median

size increased again due to the feeding of nanoalumina particles. The particle median diameter rose above 70 nm when more nanoalumina agglomerates were detected in periods IV and V.

Mobility particle size distribution

Mobility particle size distributions measured at various locations and at various times as listed in Tables 1, 2, and the cumulative count distribution in Fig. 4(b) are discussed in this section. For each measurement location and time, data concerning particle size are shown in the tables, and the particle concentration as a function of size is shown in Figs. 4(a) and 5(a). The differences in particle concentration and size distribution at various locations and times can be identified and compared from these tables and figures. Particle concentrations and the mobility size distributions were measured at the laboratory background location at four different times*, i.e.*, before warming up the machine, after warming up the machine, during feeding nanoalumina particles, and after feeding nanoalumina particles.

1) Background particle concentration and size distribution before warm-up

Particle concentration and the mobility size distribution measured before warming up the machine represent the original particles present in the laboratory air which was used as the baseline for comparison to any subsequent particle release activities. The statistical data at each second of measurement were automatically calculated by the FMPS software, and the data for one second during a stable measurement period were selected to represent the background measurement for discussion in this section. The same one second of data was selected for use in all of the tables and figures in this section. Release of airborne nanoparticle

Table 1. Particle size statistical data at background.

Particle Statistic	Background before warm-up	Background after warm-up	Background during feeding nanoalumina	Background after feeding nanoalumina
Geometric Mean, nm	38	29	54	54
Mode, nm	52	34	60	52
Geo.Std.Dev.	2.5	1.8	2.2	2.2
Total concentration, particles/cm³	1.8×10^4	3.7×10^5	4.0×10^5	4.6×10^5

Table 2. Particle size statistical data during feeding 5% nanoalumina at source and breathing zone

Particle statistic	Unit	At source	At BZ
Geo. Mean	nm	44	42
Mode	nm	190	45
Geometric Standard Deviation		3.7	1.8
Total concentration	particles/cm³	1.3×10^6	2.8×10^5

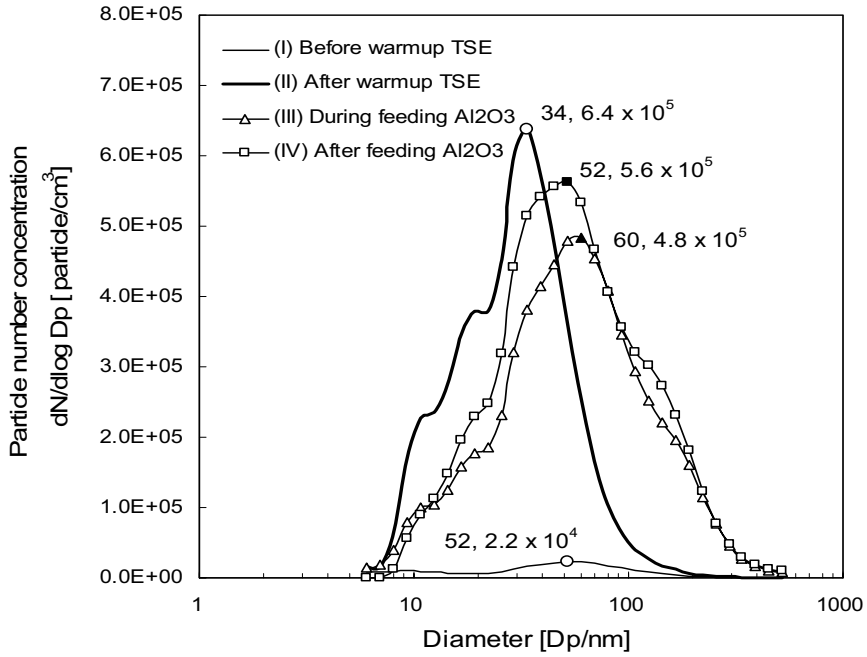

Fig. 4. (a) Instantaneous background concentration and size distribution at four different time periods.

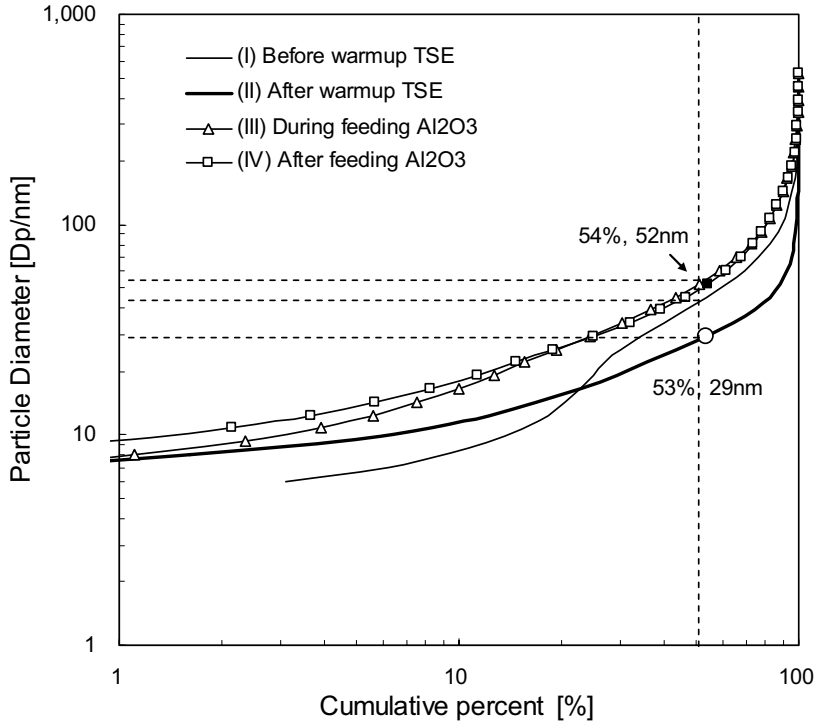

Fig. 4. (b) Cumulative count distribution on log-probability graph.

from compounding process is a fugitive process and varies considerably from second to second. The unique feature of measurement by FMPS, with its one-second sampling time, is to present the real time change of particle concentration and its size distribution. Using this characteristic, the instantaneous release of particular nanoparticles and the magnitude of release could be identified by the reading in one second. This is an advantage in using the FMPS to investigate the fugitive release of nanoparticles. For the measurement at background before warming up the TSE, the particle geometric mean size was 38 nm, the mode was 52 nm and the particle total concentration was 1.8 x 10^4 particles/cm^3 (Table 1).

As shown in Fig. 4(a), curve (I), the particle concentration was 2.2 x 10^4 particles/cm^3 at the peak particle size of 52 nm at the time before warming up the extruder. This particle size distribution and concentration represents the background airborne nanoparticles that existed in the laboratory.

2) Background particle concentration after warm up and before feeding nanoalumina

When measuring the background location after warming up the TSE, the particle geometric mean became 29 nm and the mode was 34 nm, as shown in Table 1. These diameters are smaller than those found before warming up the extruder. The count median diameter (CMD) (or geometric mean) (Hinds, 1999) of line (II) shown in Fig. 4(b) calculated based on the exposure data of curve (II) in Fig. 4(a) is consistent. The particle total concentration after warming up was 3.7 x 10^5 particles/cm^3 which is 20 fold higher than the total concentration of 1.8 x 10^4 particles/cm^3 before warming up the extruder. As shown in Fig. 4(a), curve (II), the particle concentration was 6.4 x 10^5 particles/cm^3 at the peak particle size of 34 nm after warming up the extruder which is 30 times the peak concentration before warming up the extruder.

The dramatic increase in the number of smaller nanoparticles likely was caused by the release of polymer fume and nanoparticle residues from the TSE by heating the extruder. This particle size distribution and concentration curve represents the background airborne nanoparticles that existed in the laboratory after heating the extruder but prior to feeding the nanoalumina particles and polymer.

3) Background particle concentration during the feeding of nanoalumina

For the measurement at background during feeding nanoalumina particles into the TSE, the particle geometric mean became 54 nm and the mode was 60 nm (Table 1), which are almost double the particle sizes after warming up the TSE. The concentration at the mode as seen in Fig. 4(a), curve (III) was 4.8 x 10^5 particles/cm^3; the mode was shifted to a larger value during the feeding of nanoalumina particles. In Fig. 4(b), the cumulative distribution curve shows a shift of the distribution of after warmup and during feeding Al_2O_3. That indicates more larger nanoparticles above 100 nm were distributed during feeling Al_2O_3 as seen on curve (II, III) of Fig. 4(a).

The particle total concentration during

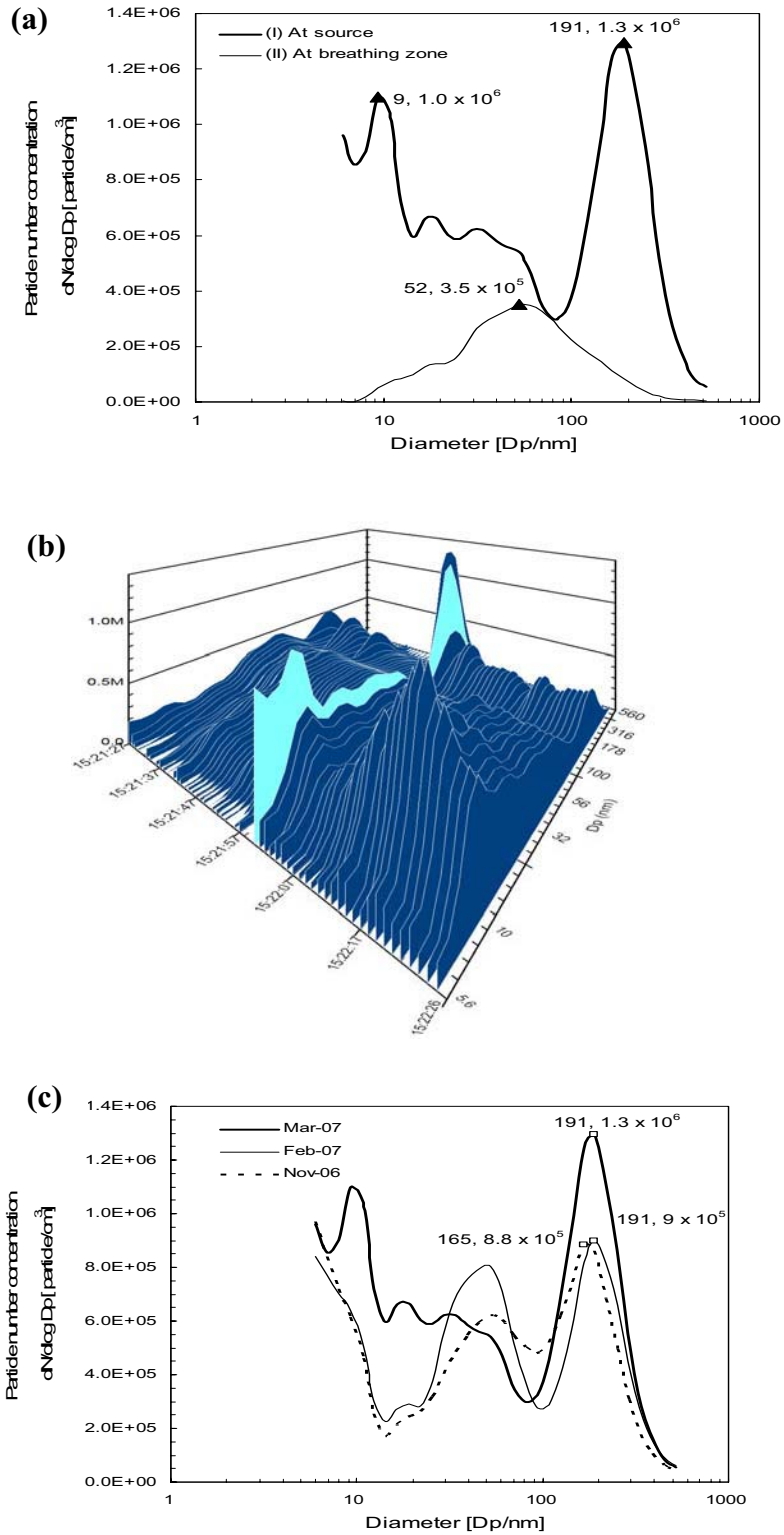

Fig. 5. Concentration and size distribution during feeding 5% nanoalumina (a) Instantaneous measurement at source and breathing zone; (b) 3D number concentration at source; (c) Instantaneous measurement at source of 3 experiments.

feeding nanoalumina was 4.0 x 10^5 particles/cm^3 as shown in Table 1 which is slightly higher than the total concentration of 3.7 x 10^5 particles/cm^3 after warming up the extruder and before feeding nanoalumina. The background concentration was dramatically increased after warming up the TSE, and the concentration remained at a high level throughout the feeding of nanoalumina particles into the TSE. In other words, the background concentration was not affected as much by the feeding of nanoalumina particles, as it was by heating the TSE. The likely reason is that the measurement location for the background concentration is 55 cm behind the extruder which is farther from the feed port than the other measurement locations. The nanoparticles released from the TSE were diffused in three-dimensional space and thus many fewer nanoparticles were carried out to the background measurement location; also, more agglomeration could have occurred during the transport of nanoparticles to the background location, which could have formed agglomerated particles having sizes beyond the measurement limit of the FMPS (560 nm).

4) Background particle concentration after feeding nanoalumina

For the measurement at the background location after feeding nanoalumina particles into the TSE, the particle geometric mean was 54 nm and the mode was 52 nm (Table 1), which are very similar to the values during feeding nanoalumina to the TSE. The concentration at the mode as seen in Fig. 4(a), curve (IV) was 5.6 x 10^5 particles/cm^3 which was reduced below the concentration after warming up the TSE. However, the count median diameters as seen in Fig. 4 (III, IV) do not have noticeable difference between lines of during and after feeding Al_2O_3.

The particle total concentration after feeding nanoalumina became 4.6 x 10^5 particles/cm^3 (Table 1), which is the highest concentration measured at the background location. Released nanoparticles during the feeding of nanoalumina particles into the TSE would agglomerate with each other and with other particles present in the air, resulting in the generation of more particles in the larger size range. This mechanism could explain the larger particle median and mode measured after the feeding process. The concentration at the background accumulated throughout the continuous feeding of nanoalumina, so that the concentration was highest at the end of feeding and it took time to gradually purge the high particle concentration by the local exhaust ventilation.

Fig. 6 shows the average data measured at the background location before and after feeding nanoalumina particles into the TSE. These curves represent the average data shown in Figs. 4(a), curves (II) and (III). The concentration measured before feeding nanoalumina is the same time as the measurement after warm up. The increased nanoparticle concentration at background through feeding nanoalumina is the difference of Fig. 4(a), curves (II) and (III) and the average data were shown in the dotted line in Fig. 6. Obviously, the concentration at background was affected by the process of

feeding nanoalumina particles. The increased particle number concentration shown in the dotted line represents the complex mixture of nanoalumina particles, PMMA fumes, residue fumes and the agglomerates of the above particles. The majority of the increased particles are in the size range of 20-200 nm.

Particle concentration and size distribution at source

The measurement at the source location during feeding nanoalumina particles into the TSE are summarized in Table 2 and Figs. 5(a), curve (I). Here, the particle geometric mean was 44 nm and the mode was 190 nm (Table 2). The total concentration at the source location was 1.3 x 10^6 particles/cm^3 (Table 2), the highest concentration measured during the experiment at any time or location, which is an order higher than the highest measurement at the background location. The concentration at the mode as seen in Figs. 5(a), curve (I) is 1.3 x 10^6 particles/cm^3 which is a large peak found only in the measurement at the source location.

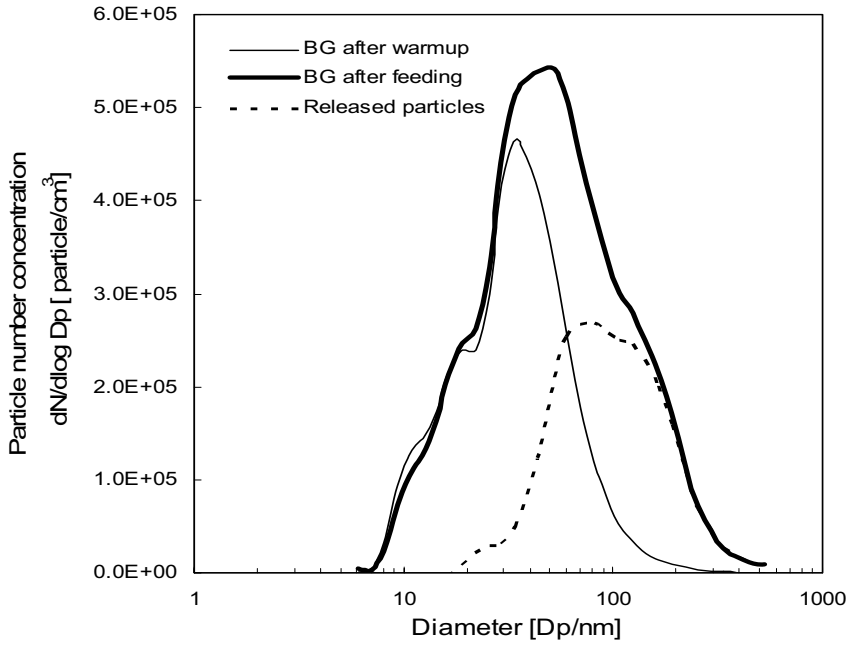

X-axis: Log scale particle diameter in nanometer, it's based on 32 channels, each channel is a range size of particles being collected. For example: channel 3.5 represents the average of particle size range of 0-7 nm

Y-axis: Normalized particle number concentration.

Note: Normalized concentration is defined as the concentration of particles in a size bin divided by the width of this bin.

If the ith bin has N_i particle concentration, thus normalized concentration in the ith bin is

$n_{Ni} = N_i / D_i$

where D_i is the width of the ith bin. For example: D_1 is 7nm

Fig. 6. Average particle number concentration and size distribution change at the room background.

The dynamic nature of the particle release is shown in Fig. 5(b), which plots the second-by-second change in the particle size distribution at the source during one location. On the other hand, the peak concentrations and distribution measured during different experiments were quite similar, as shown in Fig. 5(c), which plots the source distributions from three experiments performed under identical conditions but in different months.

The particle size distribution at the source location shows multiple peaks that have a different pattern compared to concentrations measured at other locations. The average data measured at the source location before and during feeding nanoalumina particles into the TSE is shown in Fig. 7. These curves of "BG after warm up" and "source during feeding" represent the average data shown in Figs. 4(a), curve (II) and 5(a), curve (I), respectively. The increased nanoparticle concentration at the source while feeding nanoalumina is the difference between Figs. 4(a), curve (II) and Fig. 5(a), curve (I) and the average increase in nanoparticle concentration is shown by the dotted line in Fig. 7. Released nanoparticles during feeding nanoalumina particles into the TSE at the source location caused a high concentration increase at both particle size ranges of less than 30 nm and above 50 nm.

The large increase in the concentration of nanoparticles at the source was on the order of 10^5 particles/cm^3 or greater, and the concentration of nanoparticles less than 30 nm increased by up to 3 x 10^5 particles/cm^3 at the feeding port. That more agglomerated nanoalumina particles were measured at the source location is indicated by the curve peaking at 200 nm shown in Figs. 5(a) and 7. The larger agglomerated nanoalumina particles escaping from the feeding throat contributed to the large mode of 191 nm measured at the source location.

Particle concentration and size distribution at the breathing zone

The instantaneous data of measurements at the breathing zone location during feeding nanoalumina particles into the TSE are shown in Table 2 and Fig. 5(a), curve (II); here, the particle geometric mean became 42 nm and the mode was 45 nm (Table 2) which are less than the geometric mean (54 nm) and the mode (60 nm) at the background location. The total concentration at the breathing zone location was 2.8 x 10^5 particles/cm^3 (Table 2), which is lower than the concentration of 4.0 x 10^5 particles/cm^3 at the background location during feeding nanoalumina particles. The concentration at the mode (52 nm) as seen in Figs. 5(a), curve (II) is 3.5 x 10^5 particles/cm^3 which is slightly lower than the concentration of 4.8 x 10^5 particles/cm^3 at the background location mode (60 nm).

The instantaneous particle size distribution and concentration at the breathing zone location is similar to the distribution at the background location. In addition, the average data measured at the breathing zone location before and during feeding nanoalumina particles into the TSE is shown in Fig. 8. The curve of "BZ during feeding" represents the average of over a hundred data points as shown in Fig. 5(a), curve (II). The increased nanoparticle concentration

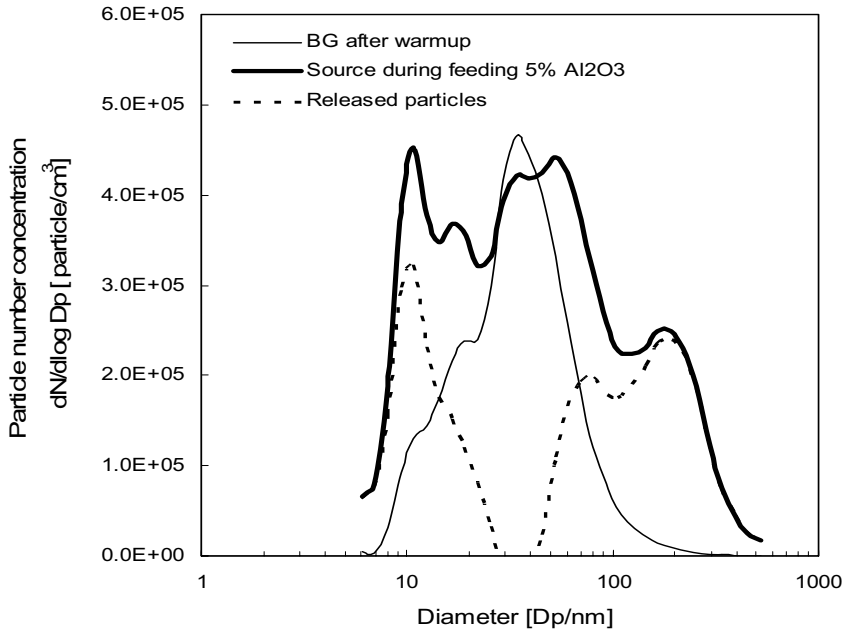

Fig. 7. Average particle number concentration and size distribution change by feeding 5% nanoalumina at the source (primary feeding port).

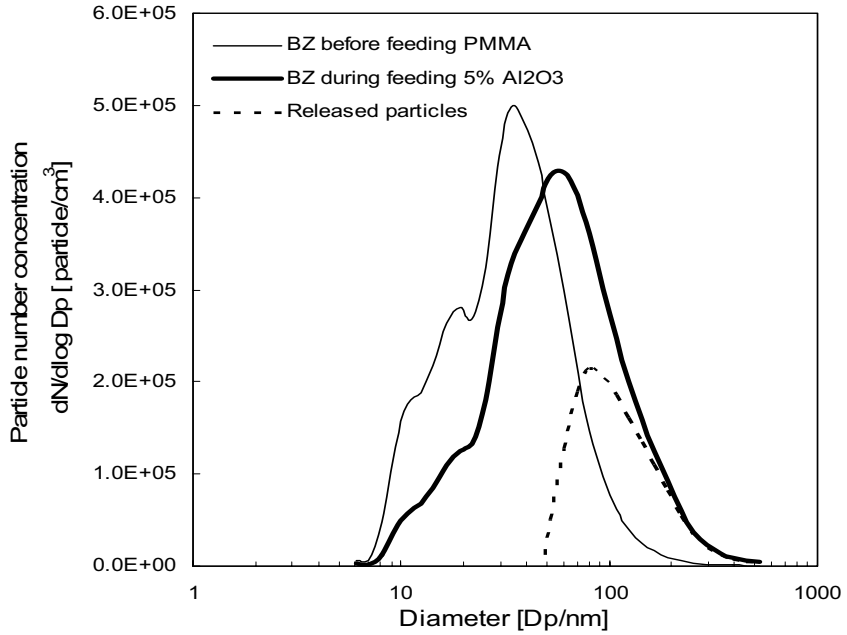

Fig. 8. Average particle number concentration and size distribution change at the breathing zone by feeding 5% nanoalumina.

at the breathing zone through feeding nanoalumina was obtained by subtracting the BZ concentration before feeding PMMA from the curve of BZ during feeding nanoalumina in Fig. 8. The increased nanoparticle concentration is shown by the dotted line in Fig. 8. Released

nanoparticles during feeding nanoalumina particles into the TSE at the breathing zone location presented similar concentration increase to the background location as seen in Fig. 6. The increased concentration of nanoparticles at the breathing zone location are in the size range of 50-200 nm with the peak concentration of 2.3 x 10^5 particles/cm^3 that was similar to the increased nanoparticles at the background location at the size range of 30-300 nm with the peak concentration of 2.5 x 10^5 particles/cm^3. There is no noticeable difference on the magnitude of exposure concentration between these two locations during feeding nanoalumina particles. That was expected as we have observed the intense circulation of airflow around the extruder which could carry nanoparticles around in the laboratory promptly. However, the particle size distribution showed the indication of size increase at the background. The increased nanoparticle mode is due to the agglomeration of the complex mixture of nanoparticles that are released into the room during the compounding and feeding processes. Thomassen *et al.* (2006) also found that nanoparticles were ageing, leading to a shift in the size distribution towards larger particles.

Overall, the characteristics of particle size and concentration at the background and the breathing zone locations are similar. However, more agglomerated nanoalumina particles were measured at the background location. Since the breathing zone location is closer to the releasing port compared to the background location, particles measured at the breathing zone would have less time to agglomerate and would be smaller than the particles at the background location.

The mixture of airborne nanoparticles

Particles collected at the source and the breathing zone locations in parallel with FMPS measurements while feeding nanoalumina are shown in Figs. 9 and 10. Collected particles on TiO_2-coated TEM grids were analyzed by STEM. A mixture of particles and aggregated nanoalumina particles collected on the TEM grid at the source can be seen on the image of Fig. 9. EDS confirmed that the light gray particles are carbon aerosols coming from the mixture of background airborne particles, likely including polymer fume particles from the heated extruder. and the dark particles are nanoalumina. A variety of nanoparticles could also be seen on the particles collected at the breathing zone as seen in Fig. 10.

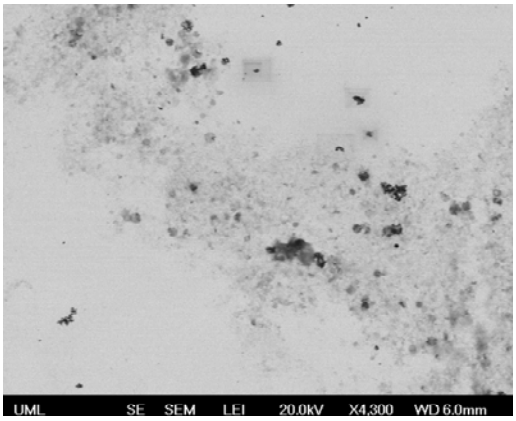

Fig. 9. SEM image of nanoparticles collected at the source.

These results indicate that the use of a size-measuring instrument such as the FMPS is insufficient to completely characterize nanoparticle aerosols composed of complex particle mixtures. A second technique, such as

the particle sampling and analysis employed in this study, is necessary to determine particle morphology and elemental composition. A challenge for the sample characterization is to quantitatively identify the size and number of nanoalumina particles and other types of nanoparticles collected on the grid. The FMPS can only measure the size distribution of the total particle mixture, without discriminating between different particle types. Further research to identify the portion of differentnanoparticles presented at the source and the breathing zone locations is necessary.

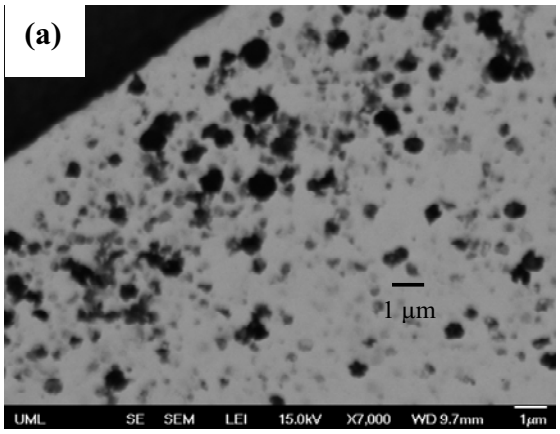

(a) Carbon and other particles

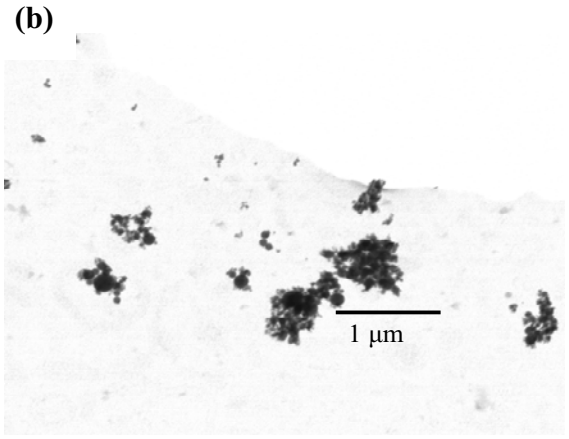

(b) Nanoalumina particles

Fig. 10. SEM images of nanoparticles collected at the breathing zone.

In addition, using only an instrument such as the FMPS, that only measures particles in the nanometer size range, would not have detected the large agglomerated particles that were formed and present in the air. This leads to the important conclusion that the measurement of particle concentration and size distribution from nanometer to micrometers is important to fully investigate the behavior of aerosols formed from processing nanoparticles.

CONCLUSIONS AND RECOMMENDATIONS

This study demonstrates conclusively that the compounding of polymers and nanoalumina in a TSE can release large quantities of nanoparticles into the air. Large quantities of nanoparticles were released during the extruder heating phase, while feeding polymer pellets only, and feeding the nanoalumina/polymer mixture. Nanoparticles released in the heating and polymer feed phases are likely to be polymer fume. When the nanoalumina particles were used instead of micrometer-size particles as fillers, the nanoparticles released during nanocompounding are a complex mixture of the individual nanoalumina particles, agglomerates of those particles, polymer fume particles, and perhaps others. Elevated nanoparticle levels were measured at the source, the room background, and the operators' breathing zone.

To adequately characterize the nanoparticle aerosols it was necessary to use both a particle size-measuring instrument (in this case, the FMPS) and a particle collection and analysis system. Further work is necessary in two areas.

First, nanocompounding variables that might influence the rate of nanoparticle release and the resulting airborne nanoparticle concentration, such as polymer and nanoparticle type, feed method, feed rate, temperature, air flow pattern, etc., must be systematically investigated. Second, the optimum sampling method to completely characterize complex nanoparticle mixtures must undergo further study and optimization.

ACKNOWLEDGEMENTS

This work was supported by the National Science Foundation as a Nanoscale Science and Engineering Centers Program (Award # NSF-0425826).

REFERENCES

Ferin, J., Oberdörster, G., Soderholm, S.C. and Gelein, R. (1991). Pulmonary Tissue Access of Ultrafine Particles. *J. Aerosol Med.-Deposit. Clear*. Effects Lung 4: 57-68.

Hinds, W. C. (1999). Aerosol Technology: properties, behavior, and measurement of airborne particles, 2nd ed. New York, Chapter 4.

Kojima, Y., Usuki, A., Kawasumi, M., Okada, A., Kurauchi, T. and Kamigaito, O. (1993). Synthesis of Nylon 6-clay Hybrid by Montmorillonite Intercalated with ε-caprolactam. *J. Polym. Sci., Part A: Polym. Chem.* 31: 983-986.

McCarrie, K.M. and Winter, R.M. (2003). Properties of Epoxy-clay Nanocomposite Adhesives for Bonded Strap Joints. *San Jose State Rep.*

Maynard, A.D. and Kuempel, E.D. (2005). Airborne Nanostructured Particles and Occupational Health. *J. Nanopart. Res.* 7: 587-614.

Renwick, L.C., Brown, D., Clouter, A. and Donaldson, K. (2004). Increased Inflammation and Altered Macrophage Chemotatic Responses Caused by Two Ultrafine Particle Types. *Occup. Environ. Med.* 61: 442-447.

Thomassen, Y., Koch, W., Dunkhorst, W., Ellingsen, D.G., Skaugset, N., Jordbekken, L., Per Arne Drablos, P.A. and Weinbruch, S. (2006). Ultrafine Particles at Workplaces of a Primary Aluminium Smelter, *J. Environ. Monit*. 8: 127-133.

Wolff, R.K., Henderson, R.F., Eidson, A.F., Pickrell, J.A., Rothenberg, S.J. and Hahn, F.F. (1988). Toxicity of Gallium Oxide Particles Following a 4-week Inhalation Exposure. *J. Appl. Toxicol.* 8: 191-199.

Warheit, D.B. (2004). Nanoparticles: Health Impacts? *Mater. Today.* 32-35.

Zhang, Q., Kusaka, Y. and Donaldson, K. (2000). Comparative Pulmonary Responses Caused by Exposure to Standard Cobalt and Ultrafine Cobalt. *J. Occup. Health.* 42: 179-184.

Received for review, January 11, 2008
Accepted, April 24, 2008